TRI-PP-86-85
Sept 1986

Cross section and analyzing power measurements for the (p,d) reaction on ^{16}O and ^{40}Ca at 200 MeV*

R. Abegg, D.A. Hutcheon and C.A. Miller

TRIUMF, 4004 Wesbrook Mall, Vancouver, B.C., Canada V6T 2A3

and

L. Antonuk†, J.M. Cameron, G. Gaillard, J.M. Greben‡, P. Kitching

R.P. Liljestrand§, W.J. McDonald, W.C. Olsen and G.M. Stinson

Department of Physics, University of Alberta,

Edmonton, Alberta, Canada T6G 2J1

and

J. Tinsley†

Physics Department, University of Oregon, Eugene Oregon 97403

†present address: Laboratoire National Saturne, CEN Saclay 91191 Gif-sur-Yvette CEDEX, France

‡present address: Theoretical Physics Division, CSIR/NR/MS, P.O. Box 395 Pretoria 0001 South Africa

§present address: EG&G Los Alamos, P.O. Box 809, 1100 4th Street, Los Alamos, NM 87544, USA.

Abstract

Cross sections and analyzing powers for the reactions $^{16}O(\vec{p},d)^{15}O$ and $^{40}Ca(\vec{p},d)^{39}Ca$ at T_p = 200 MeV have been measured to the $1/2^-$ (0 MeV) and $3/2^-$ (6.18 MeV) levels in ^{15}O and to the $3/2^+$ (0 MeV) and $1/2^+$ (2.47 MeV) levels in ^{39}Ca. Exact finite range DWBA calculations are in poor agreement with the measured angular distributions of cross sections and analyzing powers. The angular distributions of the cross sections are featureless and decrease exponentially with increasing scattering angle.

(Submitted to Physical Review C)

PACS no: 24.70.+S 25.40.Gr

*Work supported in part by the Natural Sciences and Engineering Council of Canada

I. Introduction

At low projectile energies pickup and stripping reactions have long been used to determine the angular momentum (ℓ) of the transition and the spin-parity (J^π) of the final state by comparing the angular distributions of differential cross section (σ) and analyzing power (A_y) with distorted wave Born approximation (DWBA) calculations.[1] At higher energies the specific features of A_y are, however, poorly reproduced by even exact finite range (EFR) DWBA calculations.[2,3] Cross section measurements of (p,d) reactions above about 100 MeV incident proton energy reveal angular distributions with an exponential decrease with increasing scattering angle. This decrease is essentially independent of the ℓ transfer of the transition. For example, DWBA-calculations of $^{13}C(\vec{p},d)^{12}C$ of the ground state and the 4.94 MeV transitions at 200 and 400 MeV (Ref. 2) do not reproduce the pronounced structure of the analyzing power, and fail to reproduce the flat exponential decrease of the cross section with angle. Varying the deuteron optical potential parameters for the T_p = 400 MeV study did not lead to even crude agreement with the angular distribution of the cross section. A more critical look at the comparison of EFR DWBA and measurement at 200 as well as at 400 MeV would lead one to the conclusion that the calculations cannot reproduce the angular distributions of either the cross sections or analyzing powers. At 400 MeV the situation is more complex due to Δ effects and contributions such as $NN \rightarrow \pi d$ that may play an important role. At 200 MeV such contributions are not important and therefore 200 MeV data provide a critical test of the DWBA.

In order to try to understand the disconcerting fact that the EFR

DWBA cannot reproduce data[2] at 200 MeV on $^{13}C(\vec{p},d)^{12}C$ we have extended the study of pickup reactions to ^{16}O and ^{40}Ca targets. Cross sections and analyzing powers were measured for transitions to the ground states and excited states in ^{15}O and ^{39}Ca.

II. EXPERIMENTAL PROCEDURE

A 200 MeV achromatic, polarized proton beam from the TRIUMF cyclotron was incident on targets of 151.1 mg/cm^2 thick H_2O or 50.3 mg/cm^2 thick natural Ca. The water was contained in a planar cell with thin windows of Kapton[4]. The reaction products were momentum analyzed in the 1.6 GeV/c medium resolution magnetic spectrometer (MRS). Time-of-flight and energy loss measurements allowed a clean separation of the deuterons from protons and tritons. The energy resolution of about 1.2 MeV (FWHM) was sufficient to resolve the ground states from the dominant excited states. In ^{39}Ca the 2.47 MeV level is unresolved from the 2.80 MeV ($7/2^-$) state which could contribute to the yield. In order to extract the yield the ground state line shape was used in a peak fitting procedure. The oxygen data were taken with a water target, using an empty target for background measurements. The beam current and polarization were continuously monitored using a previously calibrated in-beam polarimeter.[4]

III. EXPERIMENTAL RESULTS

The angular distributions of the cross section for the (p,d) reactions on ^{16}O and ^{40}Ca to the ground states and excited states in ^{15}O (Fig. 1) and ^{39}Ca (Fig. 2) are again rather featureless and decrease exponentially with increasing scattering angle. Confirming earlier measurements, the angular distributions of the analyzing

powers exhibit strong oscillations. The statistical errors are shown only when they are bigger than the dot size. The systematic errors are estimated to be less than 10% with the exception of the transition to the 2.47 Mev level in ^{39}Ca where they could be as high as 20%.

IV. ANALYSIS AND DISCUSSION

Optical potential parameters for the proton channel of the $^{16}O(p,d)^{15}O$ and $^{40}Ca(p,d)^{39}Ca$ reaction for zero range (ZR) and exact finite range (EFR) DWBA calculations were obtained by extrapolating the values from Ref. 5 from 135 MeV to 200 MeV using their equations. The deuteron potential was calculated by first extrapolating the proton parameters to half the deuteron energy and then utilizing the adiabatic folding approach of Wales and Johnson[6] (set a, Table 1). The ZR and EFR DWBA calculations were carried out using DWUCK4 and DWUCK 5 (Ref. 7), respectively. The Reid soft-core potential was used to generate the deuteron internal wave function and S and D waves were added coherently. The neutron form factors were calculated such that the binding energies were correct. We have also compared these calculations to predictions using recent deuteron channel parameters for $^{58}Ni(\vec{d},d)^{58}Ni$ (Ref. 8) and $^{16}O(\vec{d},d)^{16}O$ (Ref. 9) at 200 MeV as summarized in set b) of Table 1.

For ^{16}O all predictions of the angular distributions of the cross sections are similar in shape and result only in different extracted spectroscopic factors (summarized in Table II). Comparison of the predicted and observed cross sections reveals: (1) the oscillations in predicted angular distributions are more pronounced than those of the data, and (2) such oscillations as do exist in the data appear shifted

in angle with respect to those of the DWBA calculations. These discrepancies may be pointers to an incorrect weighting by our DWBA model of the contributions from large and small impact parameters. The required ℓ=1 angular momentum transfer favours small impact parameters, but the strong absorption favours the larger ones of the nuclear surface. Finite range effects do not play a role, nor is there great sensitivity to the choice of optical model parameters. The analyzing powers at forward angles are large and negative for the ground state ($j=\ell-1/2$ pick up) but near zero for the excited state ($j=\ell+1/2$). Such behaviour has previously been noted in $^{13}C(\vec{d},d)^{12}C$ at 200 MeV (Ref. 2) and $^{24}Mg(\vec{p},d)^{23}Mg$ at 150 MeV (Ref. 3). The predicted analyzing power angular distributions are not like those observed over the full angular range.

The spectroscopic factors (Table II) were extracted by normalizing to the observed cross section at the most forward angle. In view of the failure to predict the angular distributions, especially for the $^{16}O(p,d)^{15}O$(g.s.) transition, these spectroscopic factors should be treated with some caution.

For the $^{40}Ca(\vec{p},d)^{39}Ca^*$ (g.s.) transition all calculations reproduce both the angular distribution of the cross section fairly well. This is surprising in view of the fact that the parameters for the deuteron potential were taken from $^{58}Ni(\vec{d},d)$ and no scaling with energy was performed nor was the mass difference taken into account (except for the radius parameters). The extracted spectroscopic factors are similar and agree for a realistic set of deuteron potential parameters (set a) Table I) within the estimated error of 20% with published values. The transition $^{40}Ca(\vec{p},d)^{39}Ca^*$(2.47 MeV)

is not reproduced by any of the calculations. Our experiment could not resolve the 2.47 MeV ($1/2^+$) state from that at 2.80 MeV ($7/2^-$). Even though the latter has a small spectroscopic factor, it is an ℓ_n=3 pickup which is favoured over the ℓ_n=0 of the 2.47 MeV level. A definite statement on the extracted spectroscopic factor is therefore difficult to make.

V. CONCLUSIONS

We find that the angular distributions of the cross sections for the pickup reactions $^{16}O(p,d)$ and $^{40}Ca(p,d)$ at 200 MeV to the ground states and excited states in the residual nuclei are featureless and fall off exponentially with increasing scattering angle. This shape is only reproduced by the exact finite range DWBA calculation (Fig. 2) for the ground state transition in $^{40}Ca(p,d)^{39}Ca$. The extracted spectroscopic factors are in fair agreement with accepted values, although with some uncertainty in the case of $^{16}O(p,d)^{15}O$ due to the difference between the shapes of observed and calculated angular distributions. The predictions of the angular distributions of the analyzing powers when compared to data do not indicate a clear preference of the exact finite range calculations over the zero range predictions. It has been suggested[13] that increasing the proton channel spin-orbit potential (obtained from KMT) to create the oscillations necessary to fit elastic scattering data result in a good accord between DWBA and experiment at T_p = 500 MeV. In our approach we have used values that do describe elastic scattering correctly so we do not have the freedom to arbitrarily increase the spin-orbit term. The results indicate that the failure of the conventional DWBA, which was observed earlier at 150 MeV for ^{24}Mg (Ref. 3), and at 200 MeV

for ^{13}C, (Ref. 2) extends to ^{16}O at 200 MeV, but becomes less significant for larger nuclei, like ^{40}Ca. The failure of the conventional DWBA at intermediate energies for the lighter nuclei could have various causes. The recent success of Dirac approaches at higher energies[14] may suggest that the non-relativistic treatment of the distorted waves and bound-state wave functions is at fault. However, lacking a consistent relativistic theory of (p,d)-reactions it is difficult to varify this conjecture. For example, there is little virtue in modifying the proton optical potentials as suggested by the Dirac approach (like the wine-bottle shape), when one does not at the same time include the consequences of relativistic formulations for the deuteron optical potential. Since in the present study even variations in the deuteron optical potential do not change the results dramatically, the observed discrepency between theoretical and experimental results, could well hint at a breakdown of the DWBA itself, rather than at a problem in imput. Modifications of the DWBA at intermediate energies have recently been considered in the context of a microcopic distorted wave series.[15] Significant deviations from the standard DWBA were observed, however, no uniform agreement with intermediate energy data was (yet) accomplished. We conclude that further theoretical studies are necessary to establish the causes of the failure of the conventional DWBA theory to reproduce the present and previous ($\vec{p}$,d) data.

ACKNOWLEDGEMENTS

One of the authors (R.A) would like to thank Dr. A. Moalem, Bersheba University of the Negev, for fruitful and valuable discussions. We would also like to thank Dr. Nguyen van Sen, Institut des Sciences Nucléaires, Grenoble and his collaborators for sending us their unpublished deuteron channel parameters for ^{16}O at 200 MeV.

REFERENCES

[1] S.E. Vigdor, R.D. Rathmell, H.S. Liers and W. Haeberli, Nucl. Phys. A210, 70 (1973); B. Mayer, J. Gasset, J.L. Escudie and H. Kamitsubo, Nucl. Phys. A177, 205 (1971; N.S. Chant, P.S. Fisher and D.K. Scott, Nucl. Phys. A99, 669 (1967)

[2] R.P. Liljestrand, J.M. Cameron, D.A. Hutcheon, W.J. McDonald, R. Macdonald, C.A. Miller, W.C. Olsen, J.J. Kraushaar, J.R. Shepard, J.G. Rogers, J.T. Tinsley and C.E. Stronach, Phys. Lett. 99B, 311 (1981) and references therein.

[3] D.W. Miller, J.D. Brown, D.L. Friesel, W.W. Jacobs, W.P. Jones, H. Nann, P. Pichardo, J.Q. Yang, P.W.F. Alons and J.J. Kraushaar, Phys. Rev. C33, 22 (1986) and references therin.

[4] P. Kitching, C.A. Miller, W.C. Olsen, D.A. Hutcheon, W.J. McDonald and A.W. Stetz, Nucl. Phys. A340, 423 (1980).

[5] P. Schwandt, H.O. Meyer, W.W. Jacobs, A.D. Bacher, S.E. Vigdor, M.D. Kaitchuck and T.R. Donoghue, Phys. Rev. C26, 55 (1982)

[6] G.L. Wales and R.C. Johnson, Nucl. Phys. A274, 168 (1976)

[7] P.D. Kunz, University of Colorado, Boulder, Colorado 80309, Private Communication.

[8] Ngyen van Sen, J. Arvieux, Ye Yanlin, G. Gaillard, B. Bonin, A. Boudard, G. Bruge, J.C. Lugol, R. Babinet, T. Hasegawa, F. Soga, J.M. Cameron, G.C. Neilson and D.M. Sheppard, Phys. Lett. 156B, 185 (1985)

[9] Ngyen van Sen, J. Arvieux, Ye Yanlin, G. Gaillard, B. Bonin,

A. Boudard, G. Bruge, J.C. Lugol, R. Babinet, T. Hasegawa, F. Soga, J.M. Cameron, G.C. Neilson and D.M. Sheppard, Private Communication.

[10] P. Schwandt and W. Haeberli, Nucl. Phys. A110, 585 (1968)

[11] D. Bachelier, M. Bernas, I. Brissaud, C. Détraz, and P. Radvanyi, Nucl. Phys. A126, 60 (1969)

[12] I.S. Towner, Nucl. Phys. A126, 97 (1969)

[13] H. Ohnuma, F. Irom, B. Aas, M. Haji-Saeid, G.J. Igo, G. Pauletta, A.K. Rahbar, A.T.M. Wang, C.A. Whitten, Jr., M.M. Gazzaly, J.B. McClelland and T. Hasegawa, Phys. Lett. 147B, 253 (1984).

[14] J.A. McNeil, J.R. Shepard and S.J. Wallace, Phys. Rev. Lett. 50, 1439 (1983)

[15] J.M. Greben, Phys. Rev. C29, 381 (1984)

FIGURE CAPTIONS

Fig.1 Angular distributions of differential cross sections (top) and analyzing powers (bottom) for the ground state transition (left) and the transition to the excited state (right) in ^{15}O. The EFR-DWBA curve using set a) is identical to the EFR-DWBA calculation using set b) except where shown.

Fig.2 Angular distributions of differential cross sections (top) and analyzing powers (bottom) for the ground state transition (left) and the transition to the first excited state (right) in ^{39}Ca. The data for the excited state may contain contributions from a transition to the $7/2^-$ level at 2.80 MeV in ^{39}Ca which could not be resolved. The EFR-DWBA calculations using set b) are indistinguishable from the ZR calculation for the excited state transition.

Table I Optical potential parameters. The complex potential has Woods-Saxon form and is parametrized as in Ref. 10. The Coulomb potential results from a uniformly charged sphere of radius $r_c=1.3\ A^{1/3}$fm.

Reaction	Channel	V (MeV)	r (fm)	a (fm)	W_s (MeV)	r_I (fm)	a_I (fm)	V_{so} (MeV)	r_{so} (fm)	a_{so} (MeV)	W_{so} (fm)	r_{so} (fm)	A_{so} (fm)	r_c (fm)
$^{16}O(p,d)^{15}O$	p	9.44	1.41	0.60	18.72	1.03	0.68	3.77	0.88	0.63	-2.66	0.94	0.49	1.2
	a)d_1	34.61	1.32	0.68	13.60	1.49	0.57	3.97	1.00	0.42				1.3
	b)d_2	45.92	1.13	0.89	23.72	1.37	0.74	5.62	0.88	0.65				1.3
$^{40}Ca(p,d)^{39}Ca$	p	14.7	1.33	0.74	16.56	1.17	0.82	2.29	1.02	0.60	-2.35	1.00	0.62	1.2
	a)d_1	50.63	1.22	0.73	13.16	1.42	0.59	4.64	1.02	0.60	-0.97	1.00	0.62	1.3
$^{58}Ni(\vec{d},d)$	b)d_2	41.60	1.24	0.82	13.3	1.45	0.69	3.90	1.08	0.77				1.3

Table II. Summary of spectroscopic factors. a) refers to deuteron potential set a) of Table I; b) refers to the deuteron potential set b); ZR refers to spectroscopic factors obtained from the zero range calculations.

Transition	Ex (MeV)	J^π	C^2S a)	C^2S b)	C^2S ZR	C^2S ref.
$^{16}O(p,d)^{15}O$	0	$1/2^-$	1.00	1.43	0.59	1.46[c]
$^{16}O(p,d)^{15}O^*$	6.18	$3/2^-$	1.67	2.41	1.15	1.62[c]
$^{40}Ca(p,d)^{39}Ca$	0	$3/2^+$	1.96	1.41	1.34	2.58[c]
$^{40}Ca(p,d)^{39}Ca^*$	2.47	$1/2^+$	1.20	1.20	0.56	0.60[c]
$^{40}Ca(p,d)^{39}Ca^*$	2.80	$7/2^-$				0.25[c]

[c]refs. 11,12

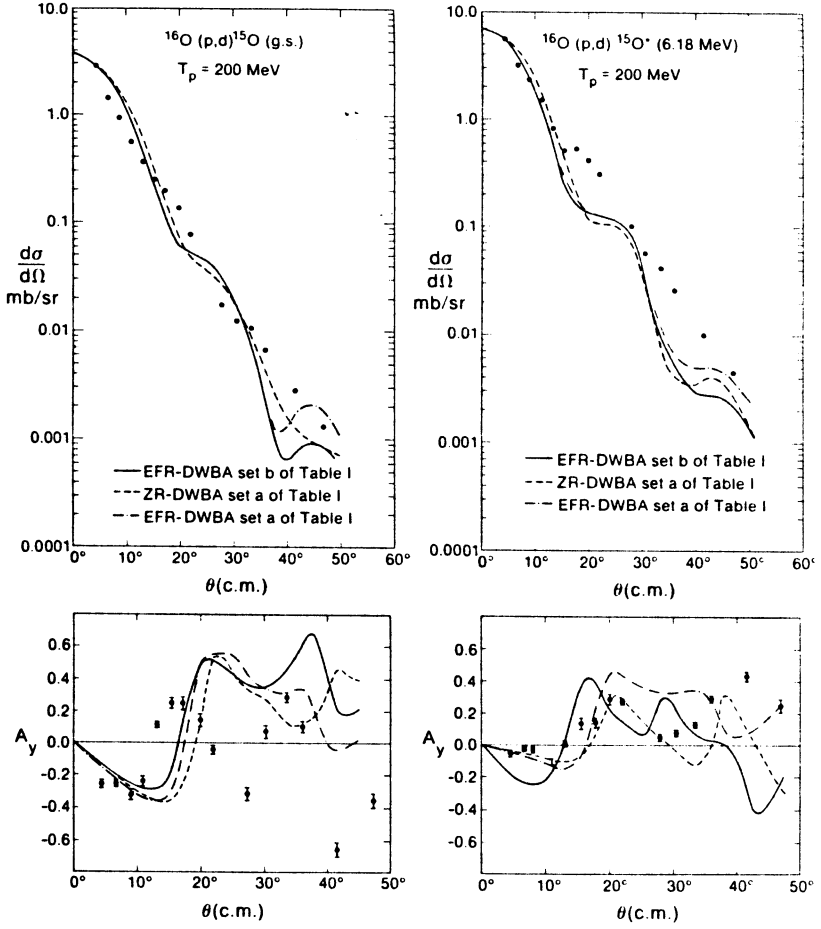
^{16}O (p,d)^{15}O (g.s.)
T_p = 200 MeV
^{16}O (p,d) ^{15}O* (6.18 MeV)
T_p = 200 MeV
EFR-DWBA set b of Table I
ZR-DWBA set a of Table I
EFR-DWBA set a of Table I
$\frac{d\sigma}{d\Omega}$ mb/sr
A_y
θ(c.m.)

Fig. 1

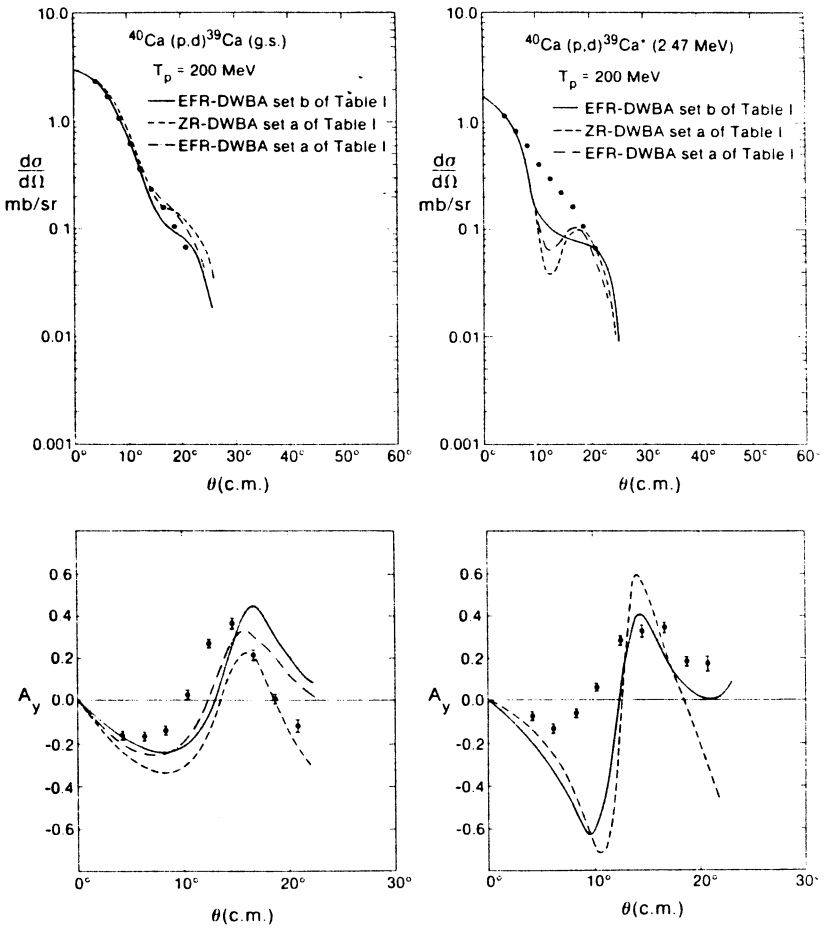
^{40}Ca (p,d)^{39}Ca (g.s.)
T_p = 200 MeV
^{40}Ca (p,d)^{39}Ca* (2 47 MeV)
T_p = 200 MeV
EFR-DWBA set b of Table I
ZR-DWBA set a of Table I
EFR-DWBA set a of Table I
$\frac{d\sigma}{d\Omega}$ mb/sr
A_y
θ(c.m.)

Fig. 2